PROCEEDINGS OF SCIENCE

JUNO potential for neutrino oscillation physics

Marco Grassi[*†]
CNRS-IN2P3, Astroparticle & Cosmology Laboratory (APC), 75013 Paris, France
CNRS-IN2P3, Linear Accelerator Laboratory (LAL), 91440 Orsay, France
E-mail: marco.grassi@mi.infn.it
on behalf of the JUNO Collaboration

The Jiangmen Underground Neutrino Observatory (JUNO) is a Liquid Scintillator (LS) detector currently under construction in the south of China (Jiangmen city, Guangdong province). JUNO aims to detect the disappearance of reactor antineutrinos at an average baseline of 53 km, with the primary goal of determining the neutrino mass ordering and performing a sub-percent measurement of three of the neutrino oscillation parameters. This physics program is rooted in the detector's capability to resolve, for the first time, the interference pattern between the solar and atmospheric oscillation modes, thanks to an unprecedented 3% energy resolution at 1 MeV.
The main purpose of this contribution is to elaborate on JUNO expected sensitivity in terms of neutrino oscillation physics, showing the impact of JUNO prospective results within the global neutrino landscape. We also address how the JUNO design is geared to achieve the target energy resolution by deploying about 18000 20-inch PMTs and 25000 3-inch PMTs to detect at least 1200 photoelectrons per MeV of deposited energy. PMTs cover 78% of the detector surface, and are arranged in a spherical geometry to monitor 20 kton of ultra-pure Linear AlkylBenzene acting as the antineutrino target mass, which make JUNO the largest LS detector currently being built. The relation between the overall detector performance and physics sensitivity will also be briefly described.

European Physical Society Conference on High Energy Physics - EPS-HEP2019 -
10-17 July, 2019
Ghent, Belgium

[*]Speaker.
[†]Now at INFN Milano, Via Celoria 16, 20133 Milano (Italy)

PoS(EPS-HEP2019)398

1. Introduction

The Jiangmen Underground Neutrino Observatory (JUNO) [1, 2] is a liquid scintillator detector currently under construction in the south of China (Jiangmen city, Guangdong province). Once completed, it will be the largest liquid scintillator detector ever built, consisting in a 20 kt target mass made of Linear Alkyl-Benzene (LAB) liquid scintillator (LS), monitored by roughly 18000 twenty-inch high-quantum efficiency (QE) photomultipliers (PMTs) providing a ∼78% photocoverage. Large photocoverage and large QE are two pivotal parameters of the experiment, which allow an unprecedented 3% energy resolution at 1 MeV. The conceptual design report [2] foresees the LS to be contained in an acrylic sphere 12 cm thick and 35.4 m wide, and the whole detector to be immersed in a cylindrical water pool, acting both as a moderator for the environmental radioactivity, and as a Cherenkov detector to tag and veto cosmic muons. A additional set of 25000 three-inch PMTs will be installed in the empty space among the twenty-inch PMTs with the goal to provide a second calorimetry handle with independent systematic uncertainties, allowing a combined more precise energy scale definition.

JUNO's main physics goal [1] is to study neutrino oscillations by detecting the disappearance reactor $\overline{\nu}_e$ produced by two nuclear power plants, both 53 km distant from the detector, with a total nominal power of 36 GW_{th} (75% of which is scheduled to be available at the beginning of the data taking). JUNO will be the first detector to observe simultaneously both solar and atmospheric oscillations, and it aims to determine the neutrino mass ordering through their interference. JUNO is also expected to measure several PMNS oscillation parameters [3] with a precision better than 1%. Moreover, JUNO has a rich physics programme focused on neutrinos not originating from reactor, described in detail in Ref. [1].

2. Neutrino Oscillation at JUNO

Nuclear power plants are pure, powerful and isotropic sources of $\overline{\nu}_e$. Recent and past experiments located at different baselines with respect to nuclear power plants successfully exploited the detection of $\overline{\nu}_e$ to prove neutrino oscillation, and to precisely measure some of the oscillation parameters [4, 5, 6, 7]. JUNO aims to detect $\overline{\nu}_e$ coming from two of the most powerful nuclear power plants in the world —Taishan and Yiangjiang, located in the Chinese province of Guangdong— to perform a precise measurement of their survival probability as a function of their energy. $\overline{\nu}_e$ detection takes place through the Inverse Beta Decay (IBD) process, where the $\overline{\nu}_e$ interacts with a proton of the liquid scintillator yielding a positron and a neutron, namely

$$\overline{\nu}_e + p \rightarrow e^+ + n.$$

The positron loses all its energy via ionization, and eventually annihilates. Such energy deposition happens instantaneously, i.e. in a timescale much shorter than the typical LS deexcitation, and is called *prompt*. On the contrary, the neutron thermalizes on a much longer time scale ($\tau \sim 200\ \mu$s) and eventually gets captured by an hydrogen of the LS, yielding a 2.2 MeV gamma (*delayed* energy deposition). Because of the mass difference between the neutron and the positron, the latter retains most of the $\overline{\nu}_e$ momentum, and the prompt energy is an accurate proxy for the $\overline{\nu}_e$ energy. The

Selection	IBD efficiency	IBD	Geo-νs	Accidental	^{9}Li/^{8}He	Fast n	(α,n)
-	-	83	1.5	$\sim 5.7\times10^4$	84	-	-
Fiducial volume	91.8%	76	1.4		77	0.1	0.05
Energy cut	97.8%			410			
Time cut	99.1%	73	1.3		71		
Vertex cut	98.7%			1.1			
Muon veto	83%	60	1.1	0.9	1.6		
Combined	73%	60	3.8				

Table 1: Signal and backgrounds daily rates, together with the efficiencies of the antineutrino selection criteria. From [1].

delayed energy deposition is a unique signal signature, and allows a powerful background rejection by means of a time and vertex correlation with respect to the prompt energy deposition.

Natural radioactivity makes up for the largest background contribution. Most of it originates from the PMT glass and from the outer wall of the detector, and is effectively reduced by applying a 0.5 m fiducial volume cut. Residual natural radioactivity events might occasionally fall within the time and vertex windows used for signal selection, yielding *accidental* coincidences which are an irreducible background. α radioactivity resulting in neutrons being ejected from stable nuclei is counted separately, and is referred to as (α,n). For the sake of reactor neutrino physics, geoneutrinos are a background affecting the low end of the energy spectrum (as shown in Fig. 1), and need to be properly subtracted. The remaining backgrounds originate from the spallation of cosmogenic muons on LS molecules. They comprise long lived isotopes (^{9}Li and ^{8}He) decaying β-n, and fast neutrons. Signal and background daily rates are summarized in Table 1.

The black line in Fig. 1 shows the expected prompt energy spectrum. It features two distinct oscillation patterns, a slow one arising from the solar mass splitting, and a fast one arising from the atmospheric mass splitting. The neutrino mass ordering information is embedded in the interference between the two oscillation modes, and can be extracted using either a Fourier-based or a χ^2-based analysis. In the following we consider the latter (a description of the former can be found in [8]), and we quantify the sensitivity to the mass ordering as the $\Delta\chi^2$ obtained from fitting the prompt energy spectrum under the two hypotheses of normal and inverted mass ordering:

$$\Delta\chi^2 = |\chi^2_{min}(\text{normal}) - \chi^2_{min}(\text{inverted})|.$$

Such a fit strongly relies on the capability to resolve the fast oscillation pattern, which in turn depends on both detector energy resolution and statistics. Fig. 2 shows $\Delta\chi^2$ contours under different assumptions of these parameters. Six years of data with an energy resolution of 3% at 1 MeV allow to reach $\Delta\chi^2 = 10$ by fitting JUNO's data alone. If we further constrain the fit using a prospective 1.5% determination of Δm^2_{ATM} at long baseline experiments, $\Delta\chi^2$ increases up to 14.

The four neutrino mixing parameters relevant to describe the JUNO energy spectrum are θ_{13}, θ_{12}, Δm^2_{12}, and either Δm^2_{31} or Δm^2_{32}. JUNO won't be able to outperform Daya Bay in the determination of θ_{13} since its baseline is optimized to be at the solar oscillation maximum, but it is expected to carry out a measurement of the remaining three parameters with a sub-percent precision. The original χ^2-based sensitivity analysis [1] shows that, taking into account shape and normalisation

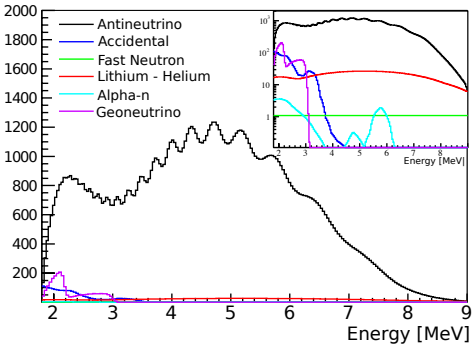

Figure 1: Energy spectra of the antineutrino signal and of the main background sources: accidental coincidences, cosmogenic ^{8}He and ^{9}Li, fast neutrons, ^{13}C$(\alpha,n)^{16}$O, and geoneutrinos. From [1].

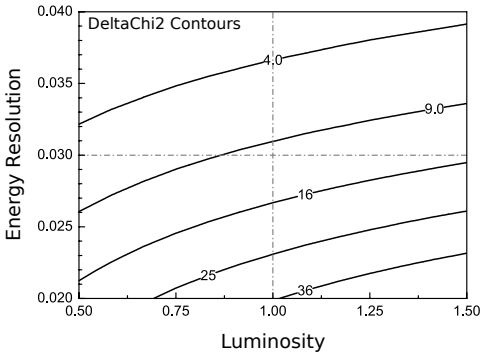

Figure 2: JUNO's sensitivity to the mass ordering determination as a function of the event statistics (luminosity) and of the detector energy resolution. Solid lines represent iso-$\Delta\chi^2$ contours. Dashed lines show the nominal runtime of six years (including 80% efficiency) and the nominal 3% energy resolution. From [1].

uncertainties due to both background and detector response, six years of data allow to determine θ_{12}, Δm^2_{12}, and a combination of Δm^2_{31} and Δm^2_{32} (i.e. Δm^2_{ee}) with a precision of 0.67%, 0.59%, 0.44% respectively. A more recent evaluation, yet to be published, seems to suggest that the actual precision will be slightly worse, but still below 1% for all the three parameters. It is worth stressing that the determination of the solar parameters depends mildly on the energy resolution, because the solar oscillation manifests itself through broad features in energy spectrum. As a consequence, such measurement can be performed even while the detector response is still being commissioned —early stage of the experiment— and, more importantly, can also be performed with the large- and small-PMT systems independently (the latter features a $\sim$15% energy resolution), allowing a powerful validation of the solar parameters determination.

3. The JUNO Detector

The JUNO detector is designed to be placed 700 m underground and comprises several components. We refer to the Central Detector as the 35.4 m wide acrylic sphere containing 20 kt of purified LAB scintillator (target volume). The target volume is monitored by 18000 20-inch PMTs

and 25000 3-inch PMTs, installed on a Stainless Steel Lattice Shell surrounding the acrylic sphere at a distance of few meters. The overall photocathode density is the largest ever built, and accounts for an unprecedented 78% photocoverage, yielding 1200 photoelectrons/MeV, pivotal to achieve the 3% energy resolution at 1 MeV. The set of large PMTs is unevenly split between dynode-based Hamamatsu Photonics PMTs, and Micro Channel Plate-based PMTs produced by the Chinese North Night Vision Technology, the latter accounting for three fourth of the total. The whole Central Detector is immersed in a cylindrical water pool filled with ultra-pure water. Since the water penetrates the Lattice Shell supporting the PMTs, it acts as a buffer shielding the target volume from natural radioactivity arising from the rock and from the PMT glass. The water pool is instrumented with about 2000 20-inch PMTs to detect Cherenkov light, hence working as an active muon veto. To better track cosmic muons, a tracker consisting of three layer of plastic scintillator (inherited from the OPERA detector [9]) is deployed on top of the water pool, covering $\sim$50% of the water pool surface. The chimney connecting the acrylic sphere to the surface of the water pool is also instrumented in order to detect stopping muons that might generate untagged background events.

The unprecedented light level of 1200 photoelectrons/MeV allows us to achieve a stochastic resolution term smaller than $2.9\%/\sqrt{E}$. However, the design resolution of 3% at 1 MeV requires to keep non-stochastic components of the energy resolution below 1%. These components mostly arise from an imperfect knowledge of the detector response, and deal with the linearity of the ionization-to-light conversion (LS response); the large dynamic range experienced by the photomultipliers (1-100 photoelectrons/channel) which affects the linearity of the light-to-charge conversion; and the uniformity of the light collection for energy deposits occurring throughout the detector volume. The latter is addressed by scanning the detector with four calibration systems: (I) one along the z axis, (II) one based on ropes deployed from the chimney and able to reach most of the off-axis region, (III) one based on a guide-tube running along the acrylic vessel to study the outermost shell of the target volume, and (IV) one based on a Remotely-Operated Vehicle to check eventual blind spots. The uncertainties arising from the LS response are addressed by deploying radioactive sources yielding neutrons and gamma lines at different energies, as well as studying the LS response with bench-top experiments. Finally, those uncertainties stemming from the linearity of the response of both PMTs and readout electronics, are addressed by means of the small-PMT system. Indeed, the PMTs' small size ensures that each phototube works in photon-counting mode, that is, on average no more than one photoelectron gets detected, effectively resulting in a *digital* calorimetry estimator. This estimator is designed to be much more robust to uncertainties typical of large phototubes, such as low-resilience to magnetic field, uniformity of the photocathode deposition, knowledge of the collection efficiency profile, pileup of multiple hits, complex waveform reconstruction, and saturation of the output signal. The small-PMT system further provides a powerful handle to help break the degeneracy existing among the three sources of systematic uncertainties. As an example, an imperfect reconstruction of the PMT waveforms experiencing large pile-up might easily mimic a residual detector non-uniformity. Such degeneracy could likely become the main limitation to a full understanding of the detector response. The study of calibration events with both the large- and the small-PMT systems, each of them providing an independent energy measurement characterized by its own hardware and reconstruction method, will allow us to sample the same energy deposition with effectively two detectors, each one experiencing a completely different systematic uncertainty budget. The comparison and the cross-calibration of these

two systems is therefore geared to become a valuable asset in understanding and minimizing the non-stochastic resolution terms.

4. Conclusions

The Jiangmen Underground Neutrino Observatory (JUNO) is a large and high precision liquid scintillator detector under construction in the south of China. With its 20 kt target mass, it aims to achieve an unprecedented 3% energy resolution at 1 MeV. To this end, a 1200 photoelectrons/MeV light level is required, which drives the effort to reach a LS attenuation length larger than 20 m, and a 78% photocoverage. Such stringent requirements are pivotal to determine the neutrino mass ordering through the analysis of $\overline{\nu}_e$ produced by two powerful nuclear power plants (36 GW_{th} nominal power) at a baseline of 53 km. The investigation of reactor $\overline{\nu}_e$ is also aimed to determine the neutrino mixing parameters θ_{12}, Δm^2_{12}, and Δm^2_{ATM} with a precision better than 1%. JUNO will further be able to detect neutrinos coming from a supernova burst, and geoneutrinos originating from the inner layers of our planet, hence extending JUNO's Physics Programme far beyond the reactor neutrino physics. Depending on the scintillator radiopurity, neutrinos originating from the Sun could also be detected, shedding light on the solar metallicity problem and on the Mikheyev-Smirnov-Wolfenstein turn on curve. JUNO's data taking is foreseen to begin in 2021.

References

[1] F. An *et al.* [JUNO Collaboration], J. Phys. G **43** (2016) no.3, 030401 [arXiv:1507.05613].

[2] F. An *et al.* [JUNO Collaboration], *JUNO Conceptual Design Report*. [*arXiv:* 1508.07166]

[3] Z.Maki *et al.*, Prog. Theor. Phys. **28** (1962) 870, B.Pontecorvo, Zh. Eksp. Theor. Fis., **53** (1967) 1717, V.Gribov and B.Pontecorvo, Phys. Lett. B **28** (1969) 493.

[4] S. Abe *et al.* (KamLAND), Phys. Rev. Lett. **100** (2008) 221803, [arXiv:0801.4589].

[5] F. P. An *et al.* (Daya Bay), Phys.Rev. D**95** (2017) 072006 [arXiv:1610.04802].

[6] Y. Abe *et al.* (Double Chooz), JHEP **01** (2016) 163, [arXiv:1510.08937].

[7] J.H. Choi *et al.* (RENO), Phys.Rev. D**98** (2018) 012002, [arXiv:1610.04326].

[8] L. Zhan, Y. Wang, J. Cao and L. Wen, Phys. Rev. D **79** (2009) 073007 [arXiv:0901.2976].

[9] R. Acquafredda *et al.* (OPERA), JINST **4** (2009) P04018.